E-ISSN: 2706-8927
P-ISSN: 2706-8919
www.allstudyjournal.com
IJAAS 2020; 2(2): 284-288
Received: 22-01-2020
Accepted: 25-02-2020

Priyaranjan
Research Scholar, Dept. of Physics, J.P. University, Chapra, Bihar, India

Corresponding Author:
Priyaranjan
Research Scholar, Dept. of Physics, J.P. University, Chapra, Bihar, India

Analysis of the ray tracing for radio propagation modeling

Priyaranjan

Abstract
Wireless communication system in the wireless channel where the radio waves are employed to carry the signals or information. This paper reviews the basic concepts of rays, ray tracing algorithms, and radio propagation modelling using ray tracing methods. We focus on the fundamental concepts and the development of practical ray tracing algorithms. The most recent progress and a future perspective of ray tracing are also discussed. We envision propagation modelling in the near future as an intelligent, accurate, and real-time system in which ray tracing plays an important role. This review is especially useful for experts who are developing new ray tracing algorithms to enhance modelling accuracy and improve computational speed.

Keywords: ray tracing, radio propagation modeling

Introduction
The simplest propagation model is the Friis equation for free space radio propagation published in 1946 [1]. It relates the received power (P_r) to the transmitted power (P_t) as a function of the distance (r) between the two antennas (assuming matched impedance and polarization) and the wavelength (λ) of the EM waves; the effect of antenna gains, G_t and G_r, is also usually included:

$$\frac{P_r}{P_t} = G_t G_r \left(\frac{\lambda}{4\pi r}\right)^2 \quad (1)$$

The received power calculated using (1) is usually referred to as the direct field from a transmitting antenna. When there exist objects protruding into the first Fresnel zone defined by the transmitter (Tx) and receiver (Rx) locations, the free space assumption fails. The reflected and/or diffracted fields have to be calculated to count the effect of the objects. These effects are often related to the reflection from ground and diffraction from mountain peaks and ridges. For the reflection, the calculation is quite simple, but the diffracted field is much more difficult to determine.
Knife edge diffraction was an important research topic in the 1940's to 1980's. Several models have been developed and are widely used. In the Bulling ton model [2, 3], several obstacles are combined into one single knife edge and the diffraction loss is then calculated in a simpler manner. Other representative models are by Epstein and Peterson [4], Deygout (an improved version) [5], and others [6]. All these methods manipulate the geometry of the wedges and ray paths to obtain approximate results. These methods all rely on the height profile of the terrain and most of the three dimensional (3D) features of the terrain are ignored.
Empirical models are widely used and are developed based on extensive field measurements. One of the most famous empirical models is the Hata-Okumura model for urban regions [7, 10]. The formula is expressed in dB units and is used to calculate the path loss L:

$$L = 10\log\left(\frac{P_t}{P_r}\right) = 69.55 + 26.16\log fMHZ - 13.82\log Hm - \alpha(h_m) + (44.9 - 6.55\log H_m)RL_{km} \quad (2)$$

where f_{MHz} is the frequency in megahertz (150MHz ≤ f_M ≤1500MHz) and R_{km} is the distance in kilometres (1km ≤ R_{km} ≤ 20km). H_m and h_m are the heights of base station and mobile unit in meters (30m ≤ H_m ≤ 200m, 1m hm ≤ 10m). The α. (h_m) term is a function of receive antenna height, frequency, and the size of the urban area. For more details, see [9, 10]. There exist extensions of the Hata-Okumura model, such as the COST-Hata-Model [15]. Other empirical models can be found in [9, 12].

Theoretical models (e.g., the Friis model and the over-rooftop diffraction model) and empirical models are in general simple and fast in terms of computation. They also have satisfactory accuracy. The main drawbacks of empirical models include that they are in general, range-based and are valid only to the environment similar to the ones from which the models are developed. Also, for recently developed multiple-input multiple-output (MIMO) systems, empirical models are not able to provide accurate space-time or angledelay results which are key characteristics for simulation of MIMO systems.

The ray tracing method, on the other hand, is based on the ray optics which solve the Maxwell's equations in high frequency regime. Thus, the ray tracing method is a general propagation modeling tool that provides estimates of path loss, angle of arrival/departure, and time delays. Unlike theoretical and empirical models, ray tracing method does not provide simple formulas for the calculation of path loss. It is a computer program and is a numerical method solving Maxwell's equations. Therefore, ray-tracing methods also belong to the computational EM (CEM) family where members such as the finite-difference time-domain (FDTD) method [13], the finite element method (FEM) [14], method of moments (MoM) [15], etc., are widely used in the design and simulation of EM systems.

Theory

The ray concept is very intuitive from our daily experience with the sun light. When the sun light goes through an opening (large compared with wavelengths) on a wall and enters the room, we can see the `ray' which is propagating along a straight line. More rigorously, the ray concept can be explained using the high frequency approximation of Maxwell's equations, see for example, [16]. The key in this explanation is the assumption that for a propagating wave, the associated electric and magnetic fields can be expressed as:

$$\vec{E}(\vec{r}) = \vec{e}(\vec{r})e^{-j\beta_0 s(\vec{r})}$$
$$\vec{H}(\vec{r}) = \vec{h}(\vec{r})e^{-j\beta_0 s(\vec{r})} \quad (3)$$

where $\vec{e}$ ($\vec{r}$) and $\vec{h}$ ($\vec{r}$) are magnitude vectors and S($\vec{r}$) is the optical path length or eikonal. Note that they are all functions of $\vec{r}$. Also the time variation in (3) is assumed harmonic and is dropped conventionally.

From Maxwell's equations with $\beta_0 \to \infty$ (high frequency regime) we have Faraday's law, Ampere's law, and Gauss' laws for electric and magnetic fields in free space (without sources):

$$L = 10\log\left(\frac{P_t}{P_r}\right) = 69.55 + 26.16\log f_{MHz} - 13.82\log H_m - \alpha(h_m) + (44,9 - 6.55\log H_m)\log R_{km} \quad (4)$$

Where, $\eta_0 = \sqrt{\frac{\mu_0}{\varepsilon_0}}$ is the impedance of free space.

We can see from the last two equations in (4) that the direction of electric and magnetic field is perpendicular to the normal direction of surfaces formed by $S = const$ (which is the wavefront surface). This normal is also the direction of the propagation direction of energy. Also, from the first equation in (4), we observe that the magnetic field has the direction determined by ∇S×e. Thus, the magnetic field is perpendicular to the electric field as well as the propagation direction. Therefore, the electric field, the magnetic field, and the propagation direction are mutually perpendicular, the same relation as in a plane wave in free space.

Eliminate $\vec{h}$ using the first two equations in (4) and with some vector algebra, we can get the eikonal equation:

$$|\nabla S|^2 = n^2 \quad (5)$$

where, $n = \sqrt{\mu_r \varepsilon_r}$ is the is the index of refraction of the medium. It can be shown by calculating the time averaged Poynting vector that the power is showing in the direction perpendicular to the wavefront surface.

To introduce the ray concept, we consider a series of wavefronts. Then we can draw the power flow lines which are perpendicular to these wavefronts. The power lines are the rays and they won't intersect if there is no focus point. Assume *ds* is a distance element along such a line. Then we can obtain the differential equation describing the power flowing line or the ray trajectory:

$$\frac{d}{ds}\left(n\frac{d\vec{r}}{ds}\right) = \nabla n \quad (6)$$

When the medium is homogeneous, i.e., ε and μ, and *n*, are constant, we have $n = 0$ and the ray trajectory equation (7) becomes,

$$\frac{d^2\vec{r}}{ds^2} = 0 \quad (7)$$

which has a solution $\vec{r} = \vec{a}s + \vec{b}$ with $\vec{a}s + \vec{b}$ with $\vec{a}$ and $\vec{b}$ being constant vectors. Thus, in homogenous medium, the ray trajectory is a straight line.

It is demonstrated in [16] that Fermat's principle of least time can be proved using the ray concept. From Fermat's principle we can obtain the laws of reflection and refraction, and even the law of diffraction [17].

The ray concept provides an effective means to understand different propagation mechanisms and a visual tool to gain insight of the interaction of EM waves. For the purpose of

radio propagation modeling using ray tracing, we summarize the ray concept as follows:

1) A ray travels in a straight line in homogeneous medium.
2) It obeys the laws of reflection and refraction, as well as the law of diffraction.
3) A ray carries energy. It is more intuitive to treat a ray as a tube (surrounding this central ray) in which the energy is contained and propagated [18].

Fig. 1 shows a ray and the associated ray tubes for a point source. Note that when a ray is traveling, the cross section of the ray tube usually increases such that the total energy or power through the cross section is constant. Equivalently, the energy density on the cross section becomes smaller as the ray travels. This effect 'spreads' the energy out and makes the field smaller when the ray travels further. The so-called *spreading factor* is used to count this effect. The electric field can also be reduced by, e.g., reflection and diffraction.

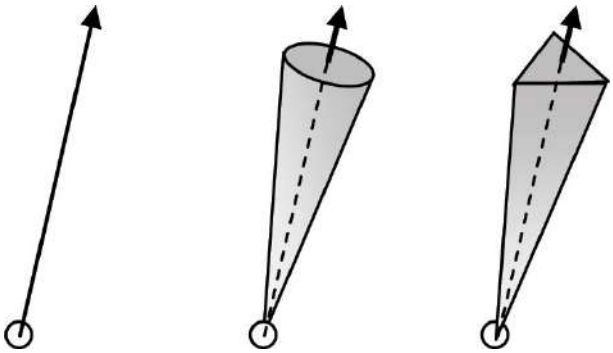

Fig 1: A ray (left) and ray tubes with circular (middle) and triangular (right) cross sections for a point source. The ray concept can also be derived without using the high frequency approximation, see [19, 20].

Diffracted Rays

Diffracted rays are more complicated compared with the direct, reflected, and transmitted rays. First, one incident ray can spawn many diffracted rays (eg. a continuum cone of rays for diffraction from a wedge). In Fig. 2, the diffracted rays from an edge are shown. For comparison, the reflected ray from an interface of two different mediums is also shown. Second, the calculation of diffraction coefficient is much more complicated than the reflection and transmission coefficients. Third, there are different formulations for the calculation of the diffraction coefficients which may give different field results. These difficulties are the reasons why we may have wide variety of methods for the calculation of diffracted field such as the knife edge method discussed in the previous section.

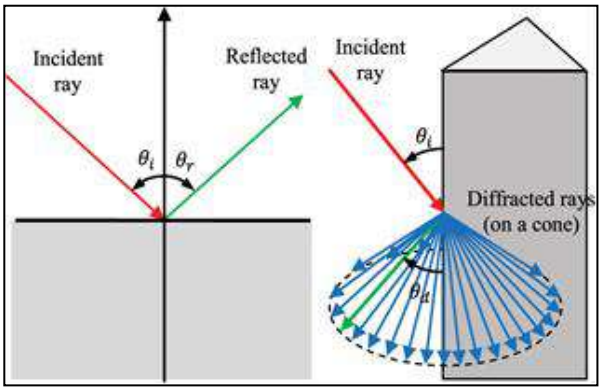

Fig 2: The reflected ray (left) from an planar interface between two different mediums and the diffracted rays (right) from an edge. Note that there is only one single reflected ray but a continuum of diffracted rays (on a cone).

The development of the geometrical theory of diffraction (GTD) and later the uniform theory of diffraction (UTD) greatly improved the accuracy for diffraction calculation for wedges. The GTD was developed by Keller in 1960's where the Fermat's principle of least time is applied to the determination of the diffracted ray path [17] and the law of diffraction was formulated: the incident angle is equal to the diffraction angle.

Scattering

Another propagation mechanism is the *scattering* from rough surfaces such as the ocean surface and building facades. For urban scenarios, the ray concept can still be used by incorporating the effect of scattering or defuse from these objects [21].

The scattering from building facades is divided into specular and nonspecular components [22]. In [23], the importance of incorporating the defuse scattering effect is validated by comparing the ray tracing simulated results with the measurement. The effective roughness concept is proposed in [24] and [25] for the calculation of scattered power form building facades. Recent developments for modelling diffuse scattering of urban environments using ray tracing can be found in [26].

Polarimetric properties of scattered power from building walls are characterized. Polynomial chaos is used in [27] to analyze the scattered field from building facades. Other approaches such as the Green's function method, near and far field method are also used in modelling the scattering from building surfaces [28, 29].

Basic ray tracing algorithms

A key part of ray tracing methods is to determine the rays from a source location to a field point. In the simplest case, i.e., in free space, the procedure is trivial: there is only one ray present (the direct ray) which is a straight line from the source to the receive point.

In an urban environment which is the most common scenario for using ray tracing, there may exist many rays from a source location to a field point; each ray may undergo different number of reflections, diffractions, or their combinations.

Image method

In Fig. 3, when the source (Tx) and the field (Rx) locations are given, the trajectory of a ray reflected from a plane surface (Σ) can be easily determined by the image method. The procedure is as follows. First, locate the image of Rx, Ri, with respect to the planar reflection surface. Second, connect Tx and Ri to obtain a line segment with intersects the plane at a point *Q*. Then, the reflected ray path is determined by three points (Tx, *Q*, Rx). Note that we can also take the image of Tx and connect Rx with the image point to obtain the same intersection point *Q*.

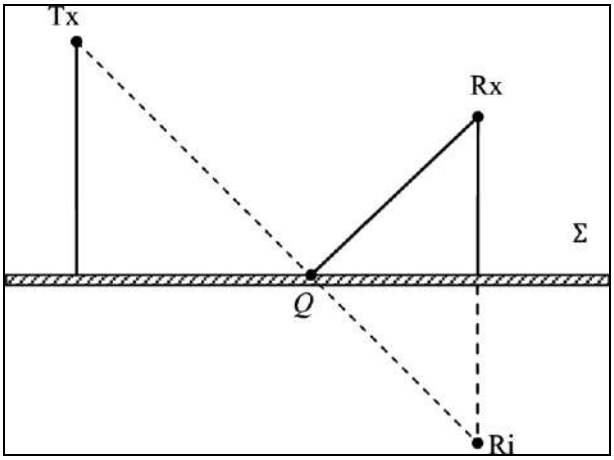

Fig 3: The image method. R_i is the image of R_x with respect to the reflection plane Σ.

The image method can be extended to determine ray path with multiple reflections. The procedure is recursive and can be implemented in a computer program conveniently.

But in a typical urban environment, the pure image method may not be efficient due to the large number of reflection surfaces, leading to slow computation speed. This is one of the reasons that the shooting and bouncing ray method is more widely used in practical propagation modeling.

Space divisions

This method is a preprocess procedure which divides the entire propagation environment into small cells. These cells have explicit or implicit information of their neighbors. When a ray traversing the environment is currently residing in a cell, the next cell the ray enters can be determined by looking up the neighboring information. This scheme reduces the number of candidate objects for the ray-object intersection tests and accelerates the computational speed.

Uniform division

The entire space of interest is divided into a uniform grid with identical cells. The cell size is constant, e.g., $dx \times dy \times dz$ for a rectangular division in three dimensional scenarios. In the preprocess, the objects in the scene will have the cells to which they belong determined and for each cell, the objects contained in the cell are calculated.

When a ray is traversing the scene, it traverses the uniform gird. In computer graphics, this traversing is well studied and fast algorithms exist. An example can be found in [30] and an application in radio propagation modeling in [31].

The key step in this algorithm is to identify the next cell the ray enters. For simplicity, we take a two-dimensional example. Assume the cell size is $\Delta_s \times \Delta_y$ and a cell is labelled by $C(i; j)$ as shown in Fig. 3. The grid lines are located at $x = i \times \Delta_x$ for vertical lines and at $y = j \times \Delta_y$ for horizontal lines.

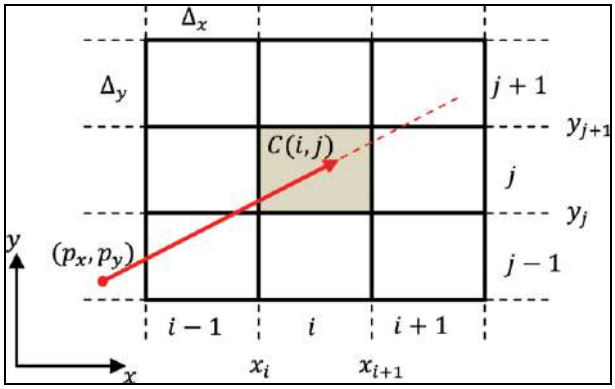

Fig 3: A rectangular grid. Each cell is a rectangle. A ray is currently residing in the cell C(i, j).

For a given ray, the ray direction can be defined by a unit vector (*ax*; *ay*). Then we can define two lengths:

$$D_x = \frac{\Delta_x}{a_x}, \quad D_y = \frac{\Delta_y}{a_y} \tag{8}$$

For $a_x \neq 0$, $a_y \neq 0$. Note that D_x is the length of the ray trajectory cut by two vertical adjacent grid lines $x = xi$ and $x = x_{i+1}$ and D_y is the length of the ray trajectory cut by two horizontal adjacent grid lines $y = y_j$ and $y = y_{j+1}$.

Then we keep two distances *dx* and *dy* which will be updated and compared to determine which cell the ray enters next from the current cell the ray is residing. Assume the source point is located at (*px*, *py*). Then the initial value of $dx = dx_0$ is the ray length cut by two lines $x = px$ and $x = xm$ (the first vertical grid line that the ray hits); the initial value of $dy = dy_0$ is the ray length cut by two lines $y = p_y$ and $y = y_n$ (the first horizontal grid line the ray hits).

The algorithm for the ray traversing can now be expressed in terms of a comparison between *dx* and *dy*:

If $dx > dy$, a horizontal grid line is traversed. The ray will go to the cell upward (or downward depending on the ray direction); update *dy* with $d_y + D_y$;

Else if $dy > dx$, a vertical grid line is traversed. The ray will go to the cell left (or right depending on the ray direction); update *dx* with $dx + Dx$.

The procedure repeats for the updated *dx* and *dy* values until some stop criterion is met.

The traversing algorithm is very fast because it only involves one addition and one comparison at each step. For each cell, the ray will be tested for intersection with any of the objects in the cell.

The rectangular grid method is extremely efficient if all the objects are aligned with the grid lines.

Conclusion

Ray tracing will play an important role in the future propagation modeling tools. In our opinion, the ray tracing method, integrated with empirical and other numerical methods (e.g., parabolic equation method), can serve as the backbone of the intelligent modeling system. It will be most useful for tackling complicated propagation environments in high frequency regimes.

References

1. Friis HT. A note on a simple transmission formula," Proc. IRE 1946;34(5):254-256.
2. Bullington K.F Radio propagation at frequencies above 30 megacycles, Proc. IRE 1947;35(10):1122-1136.
3. Propagation by Diffraction, document Rec. ITU-R 2012, 526-12. [Online]. Available: http://www.itu.int
4. Epstein J, Peterson DW. An experimental study of wave propagation at 850 Mc," Proc. IRE 1953;41(5):595-611.
5. Deygout J. Multiple knife-edge diffraction of microwaves, IEEE Trans. Antennas Propag 1966;14(4):480-489.
6. Giovaneli CL. An analysis of simplified solutions for multiple knife-edge diffraction, IEEE Trans. Antennas Propag 1984;32(3):297-310.
7. Hatay M. Empirical formula for propagation loss in land mobile radio services," IEEE Trans. Veh. Technol 1980;29(3):317-325.
8. Okumura Y, Ohmori E, Kawano T, Fukuda K. Field strength and its variability in VHF and UHF land-mobile service," Rev. Elect. Commun. Lab 1968;16(9-10):825-873.
9. Bertoni HL. Radio Propagation for Modern Wireless Systems. Upper Saddle River, NJ, USA: Prentice-Hall 2000.
10. Rappaport TS. Wireless Communications*:* Principles and Practice, 2nd ed. Upper Saddle River, NJ, USA: Prentice-Hall 2002.
11. E Damosso, LM Coreia. COST Action 231: Digital Mobile Radio Towards Future Generation Systems: Final Report, European Commission 1999.
12. Iskander MF, Yun Z. Propagation prediction models for wireless communication systems," *IEEE Trans.* Microw. Theory Techn 2002;50(3):662-673.
13. Taflove A, Hagness SC. Computational Electrodynamics: The Finite-Difference Time-Domain Method, 3rd ed. Norwood, MA, USA: Artech House 2005.
14. Jin JM. The Finite Element Method in Electromagnetics, 2nd ed. New York, NY, USA: Wiley 2002.
15. RF Harrington. Field Computation by Moment Methods. New York, NY, USA: Wiley 1993.
16. Born M, Wolf E. Principles of Optics: Electromagnetic Theory of Propagation, Interference and Diffraction of Light, 7th ed. Cambridge, U.K.: Cambridge Univ. Press 1999.
17. Keller JB. Geometrical theory of diffraction," J. Opt. Soc. Amer 1962;32(2):116-130.
18. Felsen LB, Marcuvitz N. Radiation and Scattering of Waves. Hoboken, NJ, USA: Wiley 2003.
19. Luneburg RK. Mathematical Theory of Optics. Berkeley, CA, USA: Univ. California Press 1966.
20. M Kline, Kay IW. Electromagnetic Theory and Geometrical Optics. New York, NY, USA: Interscience 1965.
21. Degli-Esposti V, A diffuse scattering model for urban propagation prediction, IEEE Trans. Antennas Propag 2001;49(7):1111-1113.
22. Pongsilamanee P, Bertoni HL. Specular and nonspecular scattering from building facades, IEEE Trans. Antennas Propag 2004;52(7):1879-1889.
23. Fuschini F, El-Sallabi H, Degli-Esposti V, Vuokko L, Guiducci D, Vainikainen P, *et al*. Analysis of multipath propagation in urban environment through multidimensional measurements and advanced ray tracing simulation," IEEE Trans. Antennas Propag 2008;56(3):848-857.
24. Degli-Esposti V, Fuschini F, Vitucci EM, Falciasecca G. Measurement and modelling of scattering from buildings, IEEE Trans. Antennas Propag 2007;55(1):143-153.
25. Lu JS, Bertoni HL, Degli-Esposti V. Scale model investigation of mechanisms for scattering from office buildings at 2 GHz, IEEE Trans. Antennas Propag 2014;62(12):6435-6442.
26. Vitucci EM, Mani F, Degli-Esposti V, Oestges C, Polarimetric properties of diffuse scattering from building walls: Experimental parameterization of a ray-tracing model, IEEE Trans. Antennas Propag 2012;60(6):2961-2969.
27. Kersaudy P, Mostarshedi S, Sudret B, Picon O, Wiart J. Stochastic analysis of scattered field by building facades using polynomial chaos, IEEE Trans. Antennas Propag 2014;62(12):6382-6393.
28. Mostarshedi S, Richalot E, Laheurte JM, Wong MF, Wiart J, Picon O, *et al.* Fast and accurate calculation of scattered electromagnetic fields from building faces using Green's functions of semi-infinite medium, IET Microw., Antennas Propag 2010;4(1):72-82.
29. Ouattara YB, Mostarshedi S, Richalot E, Wiart J, Picon O. Near- and far-field models for scattering analysis of buildings in wireless communications, IEEE Trans. Antennas Propag 2011;59(11):4229-4238.
30. JG Cleary, G Wyvill. Analysis of an algorithm for fast ray tracing using uniform space subdivision," Vis. Comput 1988;4(2):65-83.
31. Yun Z, Iskander MF, Zhang Z. Fast ray tracing procedure using space division with uniform rectangular grid, Electron. Lett 2000;36(10):895-897.